PATHOLOGICA 2025;117:588-597
DOI: 10.32074/1591-951X-1659

Original article

Immunohistochemical and molecular profiling of uveal melanoma: clinicopathological correlations from an Italian cohort

Francesco Fortarezza[1]*, Giovanni Zarrilli[2], Giada Munari[1], Valentina Angerilli[3], Mariangela Balistreri[1], Luisa Piccin[4], Valentina Salizzato[4], Jacopo Pigozzo[4], Giulia Midena[5], Raffaele Parrozzani[6], Valentina Guarneri[4,7], Edoardo Midena[5,6], Marta Sbaraglia[1,8], Matteo Fassan[8,9], Angelo Paolo Dei Tos[1,8]

[1] Surgical Pathology and Cytopathology Unit, Department of Integrated Diagnostics. Azienda Ospedale-Università Padova, Padua, Italy; [2] Surgical Pathology Unit, Azienda Ulss3 Serenissima, Ospedale dell'Angelo, Venezia, Italy; [3] Department of Surgical Pathology, Azienda ULSS2 Marca Trevigiana, Treviso, Italy; [4] Medical Oncology 2, Veneto Institute of Oncology IOV-IRCCS, Padua, Italy; [5] IRCCS-Fondazione Bietti, Rome, Italy; [6] Department of Ophthalmology, University of Padova, Padova, Italy; [7] Department of Surgery, Oncology and Gastroenterology, University of Padua, Padua, Italy; [8] Department of Medicine, University of Padua School of Medicine, Padua, Italy; [9] Veneto Institute of Oncology (IOV-IRCCS), Padua

Summary

Objective. Uveal melanoma (UM) is the most common primary intraocular malignancy in adults, characterized by distinct histopathological and molecular features and often associated with poor prognosis due to its high metastatic potential. While histology, BAP1 status, and chromosomal changes are established prognostic markers, integration of morphological, immunophenotypic, and molecular data is evolving.

Methods. We retrospectively analyzed 84 UM cases from a single institution using an integrated approach combining histological classification, immunohistochemical profiling, and targeted next-generation sequencing with a 63-gene panel. Tissue microarrays were used for immunophenotyping, and mutation data were stratified by prognostic outcomes.

Results. Most tumors were localized to the choroid and predominantly exhibited spindle-cell morphology. Mutations in *GNAQ* or *GNA11* were identified in 83% of sequenced cases. Loss of *BAP1* expression correlated with epithelioid histology and denser T-cell infiltration yet lacked PD-L1 expression. Aberrant p53 staining was more frequent in spindle-cell tumors, though *TP53* mutations were rare, suggesting functional inactivation through other mechanisms. Notably, mutations typically associated with cutaneous melanomas (e.g., *BRAF*, *KIT*, *CDKN2A*) were also detected, particularly in a single iris melanoma, suggesting site-specific molecular convergence. Additional recurrent alterations were found in *NOTCH1*, *PTEN*, *PIK3CA*, and *KDR*, implicating the mTOR and VEGF signaling pathways. A high mutational burden, along with mutations in genes such as *H3F3A*, *IDH2*, *JAK3*, and *ESR1*, was more frequent in tumors with poorer prognosis, supporting their potential role in disease aggressiveness.

Conclusions. This study highlights the heterogeneous molecular landscape of UM and underscores the importance of integrating histopathological and molecular data for improved prognostic stratification. The identification of potential therapeutic targets and atypical mutations typically associated with other melanoma subtypes suggests avenues for future research and tailored therapeutic strategies.

Key words: uveal melanoma, molecular pathology, immunohistochemistry

Received: September 10, 2025
Accepted: December 21, 2025

Correspondence
Francesco Fortarezza
E-mail: francesco.fortarezza@aopd.veneto.it

How to cite this article: Fortarezza F, Zarrilli G, Munari G, et al. Immunohistochemical and molecular profiling of uveal melanoma: clinicopathological correlations from an Italian cohort. Pathologica 2025:117:588-597. https://doi.org/10.32074/1591-951X-1659

Introduction

Uveal melanoma (UM) is the most common primary intraocular malignancy in adults[1,2]. It may arise in any of the three components of the uveal

tract: iris, ciliary body, or choroid, with the latter being by far the most frequently involved site[3]. In Caucasian populations, the incidence of UM is approximately 0.5–0.7 cases per 100,000 individuals per year[4]. The main established risk factors for UM include a low Fitzpatrick phototype, the presence of multiple nevi, oculodermal melanocytosis, and germline mutations in the *BAP1* gene[5]. The role of sunlight exposure is still debated and remains incompletely understood. The prognosis of UM remains poor. Reported survival rates at 5, 10, and 15 years are approximately 65%, 55%, and 46%, respectively[6]. The most common metastatic sites include the liver, lungs, and bones[7]. UM is considered an immunologically "cold" tumor, as immune checkpoint inhibitors have demonstrated limited efficacy. To date, tebentafusp, a bispecific T-cell engager that binds CD3 and gp100 presented by HLA A*02:01, is the only agent shown to improve overall survival in patients with metastatic UM. This classification bears prognostic relevance: epithelioid UMs are associated with the worst prognosis, while spindle-cell UMs show the most favorable outcomes[8]. Cytogenetically, UMs frequently harbor chromosomal aberrations. Commonly reported alterations include monosomy 3, gains of 8q and 6p, and loss of 1p[9]. Among these, monosomy 3 is of prognostic importance, having been linked to higher metastatic potential and poorer survival compared to disomic 3 cases. On a molecular level, approximately 90% of UMs carry mutually exclusive activating mutations in *GNAQ* or *GNA11*, which encode members of the heterotrimeric G protein alpha subunit family[10]. These alterations are not sufficient for malignant transformation, as similar mutations are also found in benign blue nevi. UMs lacking *GNAQ* or *GNA11* mutations often harbour mutations in *PLCB4* or *CYSLTR2*, which affect related signaling pathways[11]. Importantly, secondary mutations correlate with distinct clinical courses: *BAP1*-mutated UMs are commonly associated with metastasis and poor prognosis; *EIF1AX*-mutated UMs generally follow an indolent course; *SF3B1*-mutated tumors tend to have intermediate outcomes[11]. Despite these advances, the molecular landscape of UM remains incompletely understood. This study aims to investigate a large monocentric series of primary UMs, integrating histopathological, immunohistochemical, and molecular features.

Materials and methods

This study included 84 cases of primary UM diagnosed at the University Hospital of Padua between January 2010 and March 2021. All cases were reviewed by two expert pathologists, who selected representative tumor areas for molecular analysis and three tissue regions per case – two containing neoplastic tissue and one with non-neoplastic tissue – for the construction of a tissue microarray (TMA) using the Galileo CK3500 microarrayer (Integrated System Engineering). Each TMA underwent hematoxylin and eosin staining, followed by immunohistochemistry (IHC). IHC analysis was performed using the Leica Bond Max autostainer and included staining for BAP1, PD-L1, CD8, CD3, p53, MLH1, PMS2, MSH2, MSH6, and pan-TRK. Details of the antibodies, including clone, supplier, dilution, and chromogen used for immunohistochemistry, are summarized in Table I. BAP1 expression was considered positive in the presence of nuclear staining in tumor cells, and negative in its absence. p53 was classified as wild type if less than 50% of tumor cells showed nuclear staining, clonal if 50% or more were positive, and negative in cases of complete loss of staining with preserved internal controls. Mismatch repair proteins (MLH1, PMS2, MSH2, MSH6) were deemed retained if nuclear staining was strong and comparable to internal controls, lost in the complete absence of staining in tumor cells with preserved controls, and uncertain when staining was weak or discontinuous. Pan-TRK was considered positive when at least 1% of tumor cells showed nuclear, cytoplasmic and/or membranous staining of any intensity. For CD3 and CD8, the number of T lymphocytes was counted in a high-power field (40x objective, field number 22), and the lymphocytic infiltrate was considered high if over 50 lymphocytes per field were observed, or low otherwise. PD-L1 expression was evaluated by assessing the percentage of tumor cells showing membranous staining, similarly to the tumor proportion score (TPS), and by calculating the percentage of positive tumor cells, lymphocytes, and macrophages divided by the total number of viable tumor cells and multiplied by 100, in a manner similar to the combined positive score (CPS). In cases where IHC results were compromised by technical artifacts, the sample was labeled as not evaluable.

For molecular profiling, five 10-µm sections of formalin-fixed paraffin-embedded (FFPE) tissue were obtained per case. DNA extraction was performed using the QIAamp DNA FFPE Tissue Kit (Qiagen), following the manufacturer's instructions. DNA concentration was measured with the Qubit 3.0 fluorometer and the Qubit DNA BR Assay Kit (Thermo Fisher Scientific). Molecular analysis was carried out using the Archer VariantPlex Solid Tumor Panel (ArcherDX), which targets 63 genes for single nucleotide variant (SNV) detection and 44 genes for copy number variation (CNV) analysis. Only samples with adequate DNA quality,

Table I. Antibodies used for immunohistochemical analysis

Antibody	Clone	Supplier	Dilution	Chromogen
BAP1	C-4	Santa Cruz Biotechnology	1:40	Peroxidase
PD-L1	22C3	Dako	1:50	Peroxidase
CD8	4B11	Leica	1:100	Peroxidase
CD3	SP162	Abcam	1:150	Peroxidase
p53	131442	Abcam	1:100	Peroxidase
MLH1	ES05	Dako	1:50	Peroxidase
PMS2	EP51	Dako	1:40	Peroxidase
MSH2	FE11	Dako	1:50	Peroxidase
MSH6	EP49	Dako	1:50	Peroxidase
pan-TRK	EPR17341	Ventana	1:100	Peroxidase

assessed using the Archer PreSeq DNA QC assay, were processed further. Sequencing was performed on the Illumina NextSeq-550 platform. Data analysis was conducted using the Archer Analysis v6.0 software. All detected SNVs were compared with the ClinVar, Franklin by Genoox, and COSMIC databases. Only variants classified as pathogenic or likely pathogenic were included in the final analysis.

Statistical analysis was performed to assess associations between histopathological features, immunohistochemical markers, and molecular alterations. Categorical variables were compared using the χ^2 test or Fisher's exact test, as appropriate. A two-tailed p-value < 0.05 was considered statistically significant.

This study was conducted in accordance with the principles of the Declaration of Helsinki and was approved by the local Institutional Ethics Committee.

Results

The study cohort included 84 patients, with 47 males (56%) and 37 females (44%). Age at diagnosis ranged from 20 to 95 years, with a median of 68 years and a mean of 66. Tumor localization was predominantly in the choroid (79 cases, 94%), followed by the ciliary body (4 cases, 5%) and the iris (1 case, 1%). Histologically, using a 90% cellularity cutoff, 46 tumors were classified as spindle-cell (55%), 13 as epithelioid (15%), and 25 as mixed (30%) (Fig. 1). Regarding staging, 7 tumors were classified as T2 (8%), 19 as T3 (23%), and 58 as T4 (69%). Follow-up data were available for 49 patients. The mean follow-up duration was 34.3 months, with a median of 24.5 months (range: 1.3–122.3 months). Metastatic dissemination was observed in 11 cases (22%) of evaluable patients, and 6 patients (12%) died due to disease progression.

Immunohistochemical analysis revealed preserved BAP1 nuclear expression in 43 cases (54%) and loss in 36 cases (46%); 5 cases were not evaluable. For p53, 56 tumors (69%) showed a wild-type pattern, 2 (3%) were clonal, and 23 (28%) showed complete loss of expression; 3 cases were not evaluable. CD3-positive T lymphocyte infiltrate was high (> 50 lymphocytes/HPF) in 20 cases (25%), low in 60 (75%), and not assessable in 4. CD8-positive lymphocytes were high in 11 cases (14%), low in 69 cases (86%), and not evaluable in 4. Mismatch repair protein expression was retained in 76 cases (95%), uncertain in 4, and not evaluable in 4. The 4 uncertain cases underwent molecular testing and showed microsatellite stability. Pan-TRK immunostaining was negative in 76 cases (94%), uncertain in 5, and not evaluable in 3. Among the uncertain cases, molecular testing confirmed the absence of gene fusions in all but one, in which the analysis failed. PD-L1 expression was negative in all cases using both TPS and CPS. Staining with a red chromogen confirmed the absence of signal due to potential melanin interference. Representative examples of immunohistochemical expression for each marker are shown in Figure 2.

Among the 13 epithelioid cases, BAP1 expression was lost in 8, preserved in 4, and could not be evaluated in one sample. In the mixed histological subtype group, BAP1 loss was found in 12 cases, preserved in 10, and not evaluable in 3. In spindle-cell tumors, BAP1 was lost in 16 cases, preserved in 29, and not evaluable in one. However, the different BAP1 phenotype between epithelioid and spindle-cell cases did not reach the statistical significance ($p = 0.052$). p53 immunohistochemistry showed an inverted pattern. In fact, among spindle-cell tumors, 19 showed an altered expression pattern and 27 were wild-type. Among epithelioid tumors, 2 had altered expression and 10 were wild type. Also, for p53 this data did not manage to reach the statistical significance ($p = 0.1$). Analysis of CD3-positive T lymphocyte infiltration showed high infiltration in 5 epithelioid cases, low in 7, and one not evaluable. In spindle-cell tumors, 6 cases had high infiltration, 39 low, and one was not evaluable. In this case, statistical

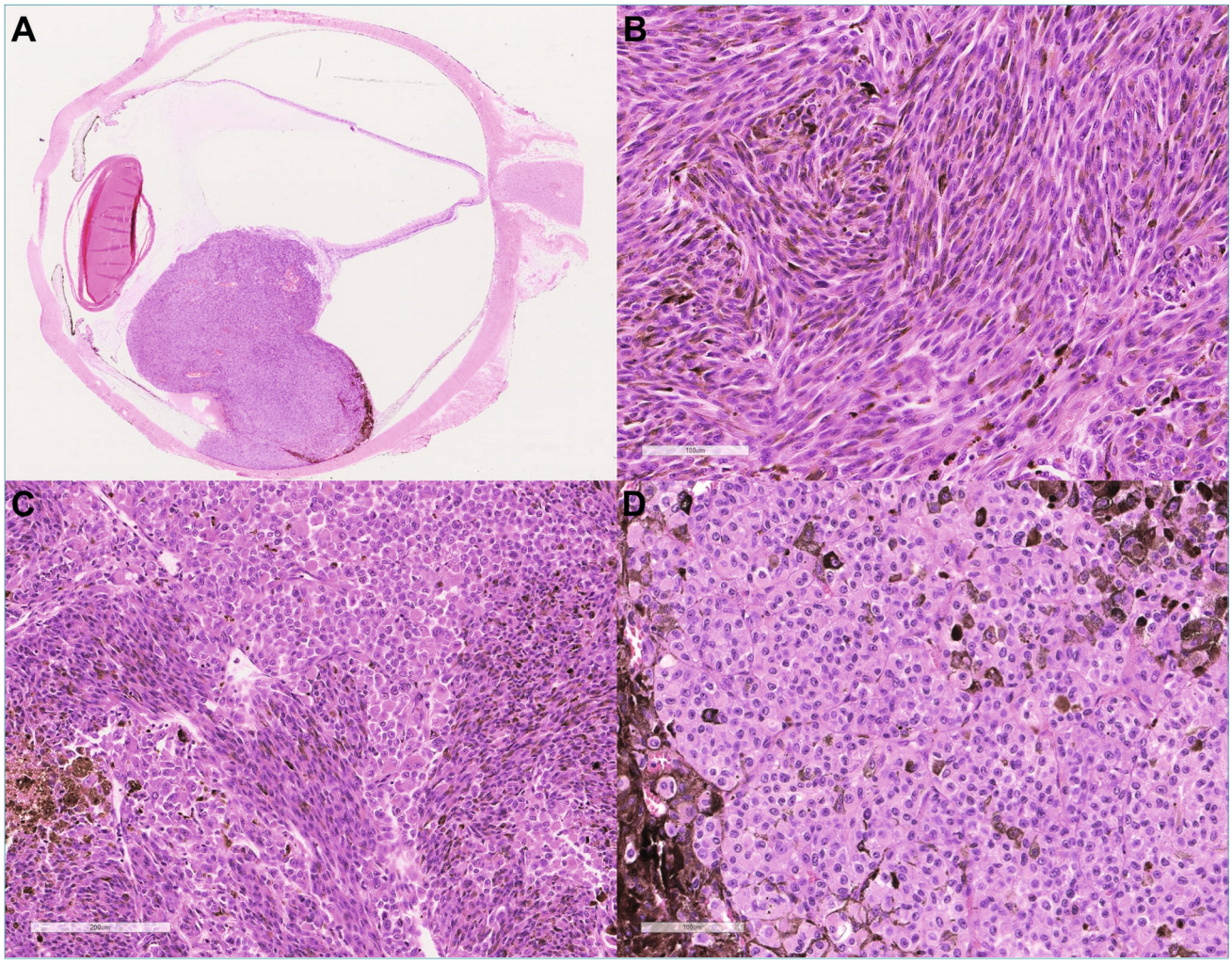

Figure 1. Panoramic view of a choroid-based uveal melanoma (A, original magnification ×10, hematoxylin and eosin stain). Spindle-cell uveal melanoma (B, original magnification ×100, hematoxylin and eosin stain). Mixed-cell uveal melanoma (C, original magnification ×100, hematoxylin and eosin stain). Epithelioid-cell uveal melanoma (D, original magnification ×100, hematoxylin and eosin stain).

significance was achieved (p = 0.027). Figure 3 illustrates the differences in immunohistochemical expression among the various histological subtypes.

Molecular testing was successfully completed in 60 of the 84 cases; the remaining 24 were excluded due to pre-analytical or technical issues. Of the cases successfully analyzed, 55 harbored at least one pathogenic or likely pathogenic variant. Mutations in *GNA11* and in *GNAQ* were identified in 29 (48%) and 21 cases (35%), respectively. All were missense variants and mutually exclusive. Only 10 cases (17%) resulted in "double negative" for the two main driver genes. *GNAQ* and *GNA11* were by far the genes with the highest frequency of SNVs. Mutations in TP53 were found in 8 cases (13%).

Interestingly, mutations commonly associated with other melanoma types were detected, including *KIT* mutations in 4 cases, *CDKN2A* in 2, and one case each with mutations in *KRAS* and *BRAF*. These mutations were mutually exclusive. The *BRAF* mutation was a V600E variant and co-occurred with partial *CDKN2A* loss. It was identified in the only case of iris melanoma.

Another interesting finding we detected was the one involving the mTOR pathway. In fact, the genes *PTEN* and *PIK3CA* were found to be altered in 2 cases each (7% globally). Furthermore, several variants of unknown significance (VUS) were found to involve these

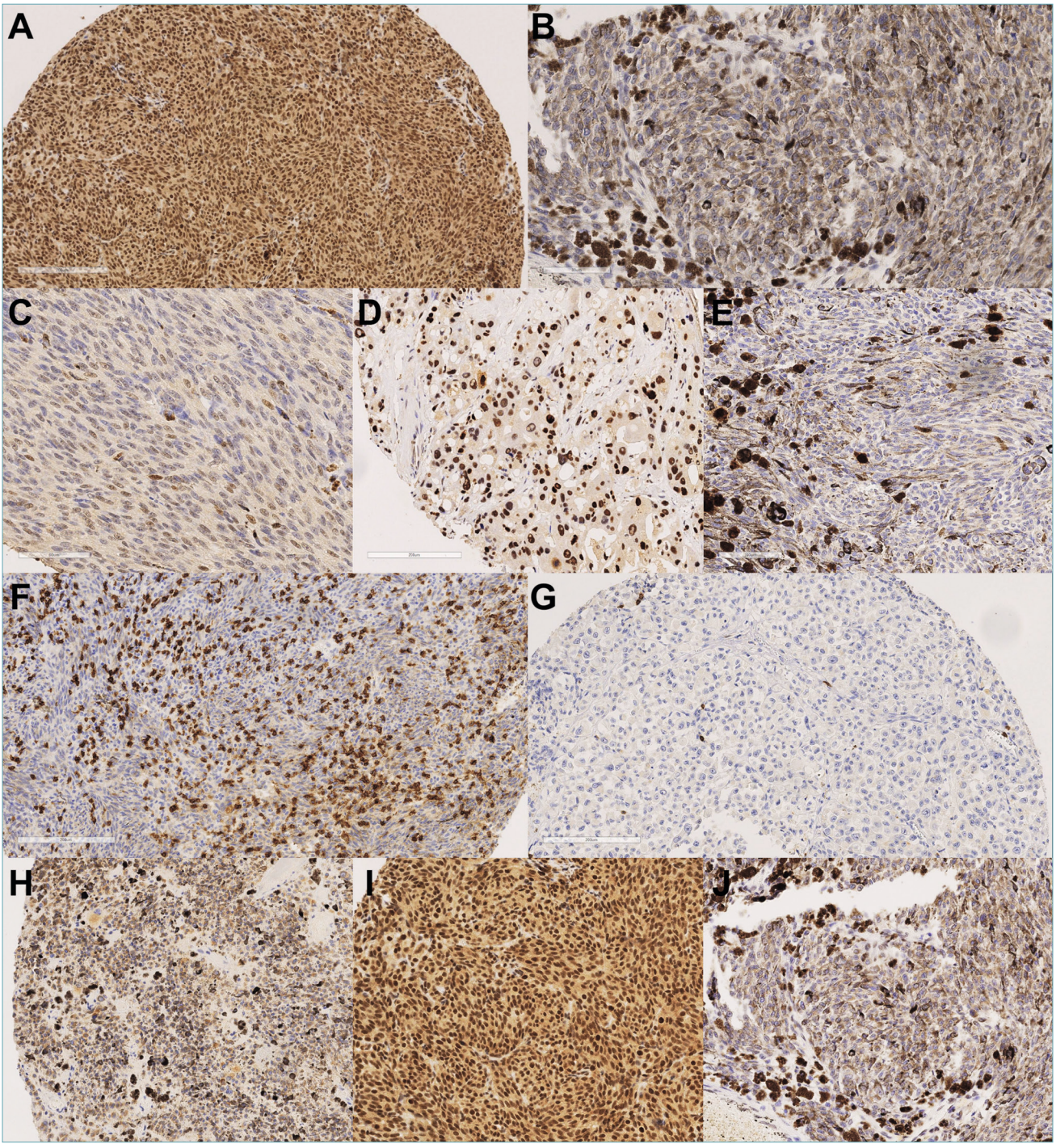

Figure 2. Representative index cases for immunohistochemical evaluation of each marker. Preserved BAP1 expression (A, original magnification ×50, peroxidase stain). Loss of BAP1 expression (B, original magnification ×100, peroxidase stain). "Wild-type" p53 expression (C, original magnification ×100, peroxidase stain). "Clonal-type" p53 expression (D, original magnification ×100, peroxidase stain). "Null-type" p53 expression (E, original magnification ×100, peroxidase stain). CD3 expression in a melanoma with abundant intratumoral lymphocytic infiltration (F, original magnification ×100, peroxidase stain). CD3 expression in a melanoma lacking intratumoral lymphocytic infiltration (G, original magnification ×100, peroxidase stain). Negative NTRK expression (H, original magnification ×100, peroxidase stain). Preserved PMS2 expression (I, original magnification ×100, peroxidase stain). Negative PD-L1 expression (J, original magnification ×100, peroxidase stain).

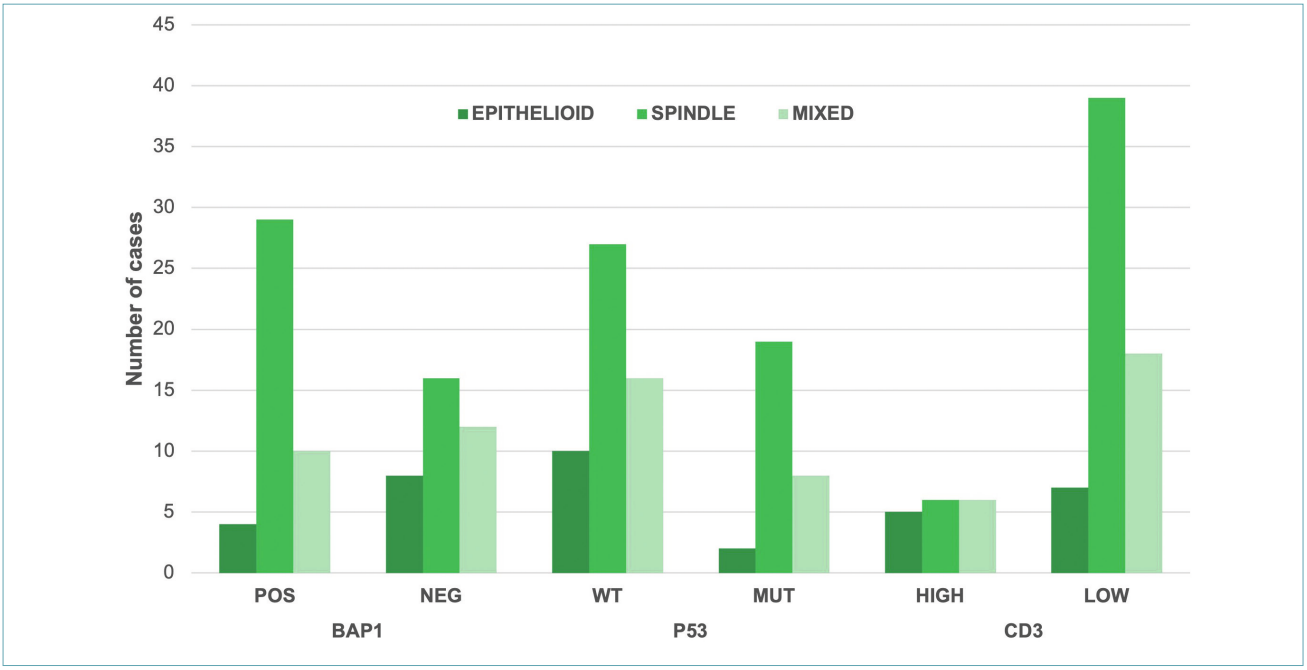

Figure 3. Distribution of immunoreactivity for BAP1, p53, and CD3 across different histological subtypes. (POS: positive; NEG: negative; WT: wild-type; MUT: mutated).

genes. In fact, *PTEN* was found to harbor VUS in 9 additional cases, while *PIK3CA* had 6 additional VUS. In total, 18 cases showed at least one molecular alteration in the genes involved in the mTOR pathway.

Among the genes analyzed, *NOTCH1* was the one with the highest incidence of VUS. In fact, *NOTCH1* showed 11 missense mutations labelled as VUS. Moreover, 3 cases with *NOTCH1* copy number variations were detected, one of which also showed a missense mutation; globally, 14 cases (23%) showed one or more alterations in *NOTCH1*.

Loss of BAP1 expression was significantly associated with an unfavorable prognosis (p = < 0.05), whereas the absence of lymphocytic infiltrate nor p53 expression did not show a statistically significant correlation with clinical outcome.

The group with the worst prognosis included 7 spindle cell cases, 2 mixed, and 2 epithelioid. The most relevant driver mutations remained *GNA11* and *GNAQ*, identified in 6 and 3 cases, respectively. Additional genes that were more frequently mutated in the poor prognosis group compared to the better one included *H3F3A* (6/11, 55% vs 1/38, 3%; $p < 0.001$), *IDH2* (3/11, 27% vs 0/38, 0%; $p = 0.01$), and *JAK3* (3/11, 27% vs 1/38, 3%; $p = 0.05$), all of which showed statistically significant differences. Other genes with higher mutation rates in the poor prognosis group, though not reaching statistical significance, were *ESR1* (3/11, 27% vs 2/38, 5%; $p = 0.12$), *FOXL2* (2/11, 18% vs 1/38, 3%; $p = 0.24$), *DDR2* (3/11, 27% vs 4/38, 11%; $p = 0.36$), *NOTCH1* (3/11, 27% vs 5/38, 13%; $p = 0.51$), *PTEN* (3/11, 27% vs 7/38, 18%; $p = 0.83$), and *MET* (2/11, 18% vs 4/38, 11%; $p = 0.87$). Among the most frequent mutations in the better prognosis group were *CDKN2A* (4/38, 10% vs 0/11, 0%, $p = 0.56$) although these differences were not statistically significant. When considering the total number of mutated genes across all cases, the poor prognosis group showed a significantly higher mutation burden compared to the better prognosis group (63/484, 13.0% vs 112/1672, 6.7%; $p < 0.001$). Figure 4 provides a comprehensive graphical representation of the molecular findings.

Discussion

This study aims to detail morphological, immunohistochemical, and molecular characteristics of a relatively large series of primary UM. The clinical features observed in our cohort, including sex distribution, age at diagnosis, and tumor localization, were consistent with existing literature.

In accordance with the multistep model of melanocytic tumor evolution proposed by the WHO panel[10], part of

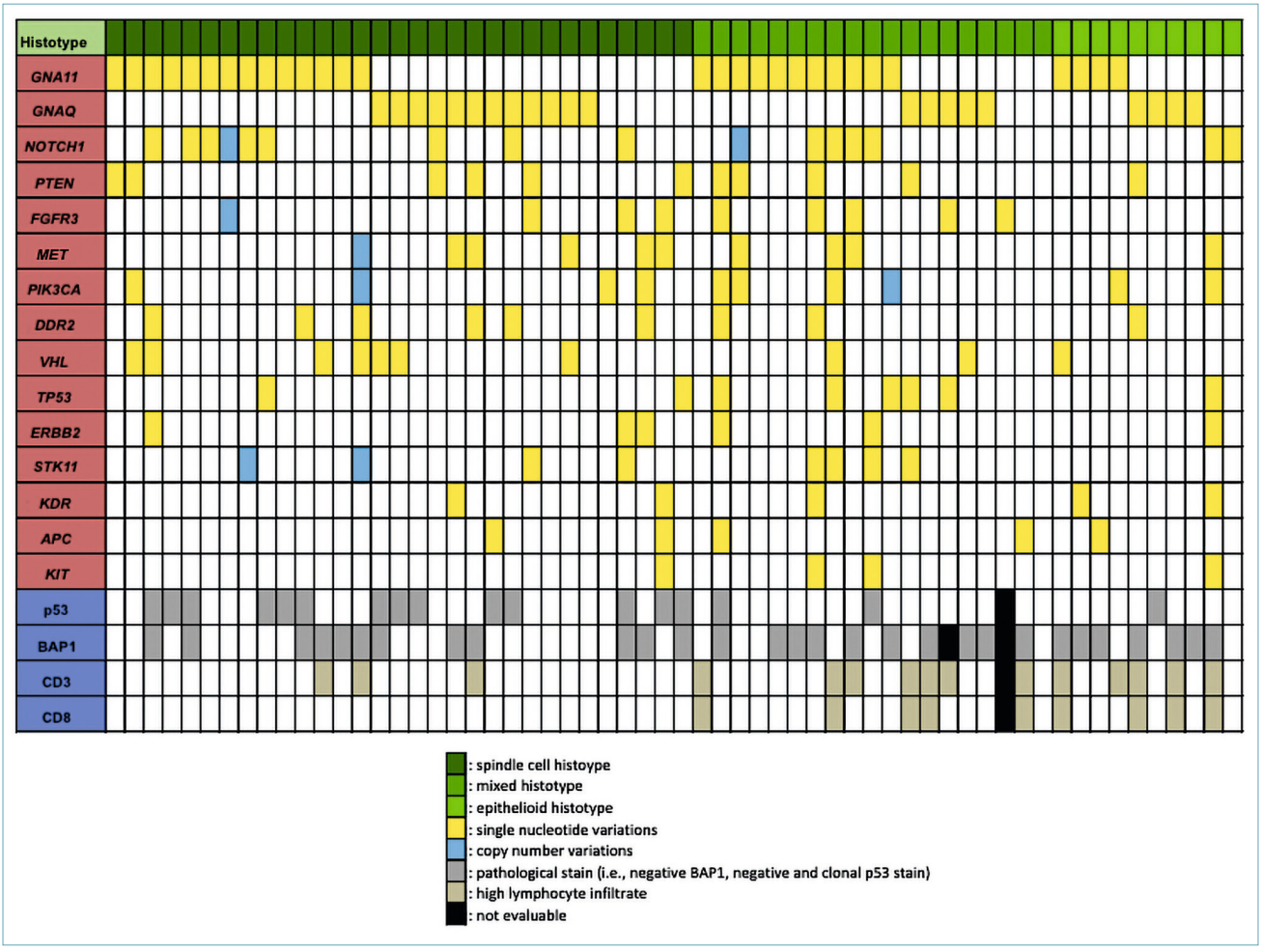

Figure 4. Representative molecular and immunohistochemical features of uveal melanoma cohort, correlated with tumor subtypes.

the genetic alterations identified in our cohort can be interpreted within a "sequence of hits" framework. The mutually exclusive mutations in *GNAQ* and *GNA11*, detected in the vast majority of cases, represent the canonical initiating events in uveal melanomagenesis and are analogous to the primary driver mutations observed in other melanocytic neoplasms. Rarely, additional melanoma-associated driver mutations typical of cutaneous melanoma may act as alternative initiating hits in specific anatomic contexts. Notably, our molecular analyses revealed that approximately 12% of cases harbored mutations of $BRAF^{V600E}$, *KIT*, *KRAS*, and *CDKN2A*. Their presence in uveal melanomas raises the question of whether such alterations might represent true pathogenetic drivers in this context or rather passenger mutations with limited functional impact. Interestingly, the only case of iris melanoma in our cohort showed a $BRAF^{V600E}$ mutation in the absence of alterations in *GNAQ* or *GNA11*. The same case also showed a *CDKN2A* mutation, which is rarely observed in UM and represents a typical second hit in cutaneous melanomagenesis. This finding is consistent with previous reports in the literature suggesting that melanomas of the iris may be more susceptible to ultraviolet radiation-induced mutagenesis, thereby aligning them more closely with cutaneous melanoma from a molecular standpoint.

Progression-related alterations, by contrast, were more heterogeneous and included genes with recognised roles in UM biology and aggressive clinical behavior. Chief among these was BAP1, whose loss of nuclear expression was more frequently observed in epithelioid UM than in spindle-cell variants and was also more common in the unfavorable prognosis group. This observation aligns with prior literature and reinforces the well-established association

between *BAP1* inactivation and poor prognosis in UM[12]. Immunohistochemistry for BAP1 thus remains a practical surrogate for identifying biologically aggressive tumors[13]. However, it should be noted that rare cases of UM with *BAP1* mutations[14], as well as cutaneous BAP1-inactivated melanocytomas[15], have been reported to retain BAP1 immunoreactivity. Such discrepancies may result from truncated BAP1 proteins that remain detectable by the antibody, from intratumoral heterogeneity with residual BAP1-competent cell populations, or from undetected intronic or complex genomic alterations preventing complete loss of protein expression. Both epithelioid morphology and BAP1-negative status were associated with increased numbers of tumor-infiltrating lymphocytes, confirming the role of *BAP1* in shaping the tumor immune microenvironment[16]. This finding stands in sharp contrast to what is typically observed in cutaneous melanoma, where a dense lymphocytic infiltrate generally correlates with improved prognosis. A statistically significant correlation was found between histological subtype and CD3-positive T lymphocyte infiltration, with epithelioid UMs exhibiting denser infiltrates. Moreover, despite the presence of T cells, none of the tumors, regardless of infiltration density, showed PD-L1 expression. This absence suggests an ineffective or non-functional immune response in the UM microenvironment, potentially explaining the limited efficacy of immune checkpoint inhibitors in this tumor type. Interestingly, the immunohistochemical expression of p53 displayed an inverse trend compared to that of BAP1. Spindle cell melanomas, which are generally considered less aggressive, more frequently exhibited a mutated p53 immunophenotype. In contrast, epithelioid melanomas – associated with poorer prognosis and typically showing loss of *BAP1* – tended to retain a wild-type pattern of p53 expression. The unexpected mismatch between tumor morphology and p53 immunoreactivity indicates that the p53 pathway in UM is regulated differently from other melanoma subtypes. Although the p53 pathway is functionally suppressed in UM, true *TP53* mutations are rare; instead, p53 inactivation may be the result of alternative mechanisms, most notably the overexpression of *MDM2* and *BCL2*[17].

Additional mutations identified included *KDR*, components of the PI3K/AKT/mTOR pathway (such as *PTEN* and *PIK3CA*), *NOTCH1*, and several genes enriched in the poor-prognosis subgroup, including *H3F3A*, *IDH2*, *JAK3*, *ESR1* and *MET*.

KDR encodes the Vascular Endothelial Growth Factor Receptor 2 (VEGFR2)[18], whose principal ligand is VEGF-A. The role of the VEGF/VEGFR axis has been rarely explored in UM. However, one study reported the expression of both VEGFR1 and VEGFR2 in UM cell lines and demonstrated a reduced proliferation rate following treatment with bevacizumab, a monoclonal antibody that targets VEGF-A[19].

Our findings highlight the potential involvement of the PI3K/AKT/mTOR pathway in the pathobiology of UM. While clearly pathogenic mutations in *PTEN* and *PIK-3CA* were limited, the frequent detection of variants of uncertain significance suggests broader, possibly subclinical, dysregulation of this pathway. These results align with recent evidence identifying UM subtypes with poor prognosis characterized by activation of the PI3K/AKT/mTOR axis, inflammatory signaling, and immune checkpoint upregulation[20].

The notable frequency of *NOTCH1* alterations observed in our cohort highlights a potentially underexplored avenue in the molecular landscape of uveal melanoma. Emerging evidence suggests that *NOTCH1* signaling may enhance tumor aggressiveness, possibly by engaging oncogenic cascades such as the AKT/mTOR, MAPK/ERK, and JAK/STAT pathways. *In vitro* data further support this notion, demonstrating that pharmacological inhibition of the NOTCH pathway can attenuate tumor growth and invasiveness in UM cell models[21].

Mutations in *H3F3A*, a key regulator of chromatin remodeling, are known drivers of aggressive behavior in pediatric gliomas[22], although their direct role in UM remains unclear. *IDH2* mutations, well documented in hematologic malignancies and gliomas[23], are rare in UM yet may still hold prognostic relevance. Analyses of TCGA and GEO datasets identified *IDH2* among four genes associated with high $CD8^+$ T-cell infiltration – paradoxically linked to worse prognosis in UM – suggesting a role in shaping an ineffective or immunosuppressive tumor microenvironment[24]. Although *JAK3* mutations are poorly characterized in UM, the documented activation of the JAK/STAT pathway in this tumor type implies that *JAK3* alterations could contribute to tumor progression and immune evasion[25,26]. The increased frequency of *ESR1* mutations in poor-prognosis UM, together with evidence of estrogen receptor expression and elevated *ESR1*/*ESR2* transcription in genetically unfavorable tumors[27], supports a pathogenic role for estrogen-receptor signaling and its potential as a therapeutic target. Finally, the enrichment of *MET* mutations in the poor-prognosis subgroup underscores the importance of signalling driven by hepatocyte growth factor (HGF) in UM progression and liver metastasis. This finding is consistent with the adaptation of *MET*-altered tumor cells to the HGF-rich hepatic environment, reinforcing *MET* as both a prognostic marker and a potential therapeutic target[28].

As with any research, this study has certain limitations. First, its retrospective nature may have introduced biases in sample selection and data interpretation and limited the availability of clinical follow-up and survival data. Secondly, although we employed a broad multigene panel, it did not include several genetic alterations known to play key roles in UM biology and prognosis, such as *SF3B1* and *EIF1AX*. Furthermore, copy number variations in chromosomes 3 and 8q—well-established markers of prognosis in UM—were not systematically evaluated.

Nonetheless, we believe that the insights generated by our integrative approach offer valuable new perspectives on this rare malignancy. The identification of atypical mutational profiles, immune microenvironment features, and potential therapeutic targets underlines the importance of expanding the molecular and immunohistochemical assessment of UM. Future prospective, multicenter studies incorporating broader molecular panels and clinical outcome data are warranted to validate these findings and explore their translational implications.

Conflicts of interest statement

The authors declare no conflict of interest

Funding

The authors declare that no financial support was received for the research, authorship, and/or publication of this article.

Authors' contributions

FF, MF, APDT conceived and designed the study. GM and MB performed the histological and immunohistochemical analyses. GM, MB carried out the molecular investigations. FF performed the statistical analyses. Data collection and curation were done by GZ, VA, LP, VS, JP, GM, RP. FF and GZ drafted the initial version of the manuscript. FF, MF, APDT, MS, VG, EM and RP critically revised and edited the manuscript. APDT supervised the project and provided overall guidance. All authors read and approved the final version of the manuscript.

Ethical consideration

The research was conducted ethically, with all study procedures being performed in accordance with the requirements of the World Medical Association's Declaration of Helsinki and was approved by the local Institutional Ethics Committee. Written informed consent was obtained from each participant/patient for study participation and data publication.

References

1 Spagnolo F, Caltabiano G, Queirolo P. Uveal melanoma. *Cancer Treat Rev*. 2012;38(5):549-553. https://doi.org/10.1016/j.ctrv.2012.01.002

2 Chang AE, Karnell LH, Menck HR. The National Cancer Data Base report on cutaneous and noncutaneous melanoma: a summary of 84,836 cases from the past decade. The American College of Surgeons Commission on Cancer and the American Cancer Society. *Cancer*. 1998;83(8):1664-1678. https://doi.org/10.1002/(sici)1097-0142(19981015)83:8 < 1664::aid-cncr23 > 3.0.co;2-g

3 Damato B. Treatment of primary intraocular melanoma. *Expert Rev Anticancer Ther*. 2006;6(4):493-506. https://doi.org/10.1586/14737140.6.4.493

4 Hu DN, Yu GP, McCormick SA, Schneider S, Finger PT. Population-based incidence of uveal melanoma in various races and ethnic groups. *Am J Ophthalmol*. 2005;140(4):612-617. https://doi.org/10.1016/j.ajo.2005.05.034

5 Yonekawa Y, Kim IK. Epidemiology and management of uveal melanoma. *Hematol Oncol Clin North Am*. 2012;26(6):1169-1184. https://doi.org/10.1016/j.hoc.2012.08.004

6 Singh M, Durairaj P, Yeung J. Uveal Melanoma: A Review of the Literature. Oncol Ther. 2018 Jun;6(1):87-104. https://doi.org/10.1007/s40487-018-0056-8. Epub 2018 Feb 6. Erratum in: Oncol Ther. 2019 Jun;7(1):93. https://doi.org/ 10.1007/s40487-019-0093-y. PMID: 32700136; PMCID: PMC7359963.

7 Mariani P, Torossian N, van Laere S, Vermeulen P, de Koning L, Roman-Roman S, Lantz O, Rodrigues M, Stern MH, Gardrat S, Lesage L, Champenois G, Nicolas A, Matet A, Cassoux N, Servois V, Romano E, Piperno-Neumann S, Lugassy C, Barnhill R. Immunohistochemical characterisation of the immune landscape in primary uveal melanoma and liver metastases. Br J Cancer. 2023 Sep;129(5):772-781. https://doi.org/ 10.1038/s41416-023-02331-w. Epub 2023 Jul 13. PMID: 37443346; PMCID: PMC10449826.

8 Shields CL, Kaliki S, Furuta M, Fulco E, Alarcon C, Shields JA. American Joint Committee on Cancer classification of posterior uveal melanoma (tumor size category) predicts prognosis in 7731 patients. *Ophthalmology*. 2013;120(10):2066-2071. https://doi.org/10.1016/j.ophtha.2013.03.012

9 Robertson AG, Shih J, Yau C, et al. Integrative Analysis Identifies Four Molecular and Clinical Subsets in Uveal Melanoma [published correction appears in Cancer Cell. 2018 Jan 8;33(1):151. https://doi.org/ 10.1016/j.ccell.2017.12.013.]. *Cancer Cell*. 2017;32(2):204-220.e15. https://doi.org/10.1016/j.ccell.2017.07.003

10 Fortarezza F, Cazzato G, Ingravallo G, Dei Tos AP. The 2023 WHO updates on skin tumors: advances since the 2018 edition. Pathologica. 2024;116(4):193-206. https://doi.org/10.32074/1591-951X-1006

11 Păsărică MA, Curcă PF, Dragosloveanu CDM, Grigorescu AC, Nisipașu CI. Pathological and Molecular Diagnosis of Uveal Melanoma. Diagnostics (Basel). 2024 May 2;14(9):958. https://doi.org/ 10.3390/diagnostics14090958. PMID: 38732371; PMCID: PMC11083017.

12 Matull J, Placke JM, Lodde G, Zaremba A, Utikal J, Terheyden P, Pföhler C, Herbst R, Kreuter A, Welzel J, Kretz J, Möller I, Sucker A, Paschen A, Livingstone E, Zimmer L, Hadaschik E, Ugurel S, Schadendorf D, Thielmann CM, Griewank KG. Clinical and genetic characteristics of *BAP1*-mutated non-uveal and uveal melanoma. Front Immunol. 2024 Jun 5;15:1383125. https://doi.org/ 10.3389/fimmu.2024.1383125. PMID: 38903495; PMCID: PMC11188379.

13 Han LM, Lee KW, Uludag G, et al. Prognostic Value of BAP1 and Preferentially Expressed Antigen in Melanoma (PRAME) Immunohistochemistry in Uveal Melanomas. *Mod Pathol*. 2023;36(4):100081. https://doi.org/10.1016/j.modpat.2022.100081

14 Koopmans AE, Verdijk RM, Brouwer RW, et al. Clinical significance of immunohistochemistry for detection of BAP1 mutations

in uveal melanoma. Mod Pathol. 2014;27(10):1321-1330. https://doi.org/10.1038/modpathol.2014.43

15 Linos K, Atkinson AE, Yan S, Tsongalis GJ, Lefferts JA. A case of molecularly confirmed BAP1 inactivated melanocytic tumor with retention of immunohistochemical expression: A confounding factor. J Cutan Pathol. 2020;47(5):485-489. https://doi.org/10.1111/cup.13642

16 Figueiredo CR, Kalirai H, Sacco JJ, Azevedo RA, Duckworth A, Slupsky JR, Coulson JM, Coupland SE. Loss of BAP1 expression is associated with an immunosuppressive microenvironment in uveal melanoma, with implications for immunotherapy development. J Pathol. 2020 Apr;250(4):420-439. https://doi.org/ 10.1002/path.5384. PMID: 31960425; PMCID: PMC7216965.

17 Shin JS, Ha JH, Chi SW. Targeting of p53 peptide analogues to anti-apoptotic Bcl-2 family proteins as revealed by NMR spectroscopy. *Biochem Biophys Res Commun*. 2014;443(3):882-887. https://doi.org/10.1016/j.bbrc.2013.12.054

18 Li B, Ogasawara AK, Yang R, et al. KDR (VEGF receptor 2) is the major mediator for the hypotensive effect of VEGF. *Hypertension*. 2002;39(6):1095-1100. https://doi.org/10.1161/01.hyp.0000018588.56950.7a

19 Yang H, Jager MJ, Grossniklaus HE. Bevacizumab suppression of establishment of micrometastases in experimental ocular melanoma. *Invest Ophthalmol Vis Sci*. 2010;51(6):2835-2842. https://doi.org/10.1167/iovs.09-4755

20 Geng Y, Geng Y, Liu X, et al. PI3K/AKT/mTOR pathway-derived risk score exhibits correlation with immune infiltration in uveal melanoma patients. *Front Oncol*. 2023;13:1167930. Published 2023 Apr 20. https://doi.org/10.3389/fonc.2023.1167930

21 Asnaghi L, Ebrahimi KB, Schreck KC, et al. Notch signaling promotes growth and invasion in uveal melanoma. *Clin Cancer Res*. 2012;18(3):654-665. https://doi.org/10.1158/1078-0432.CCR-11-1406

22 Zhang R, Han J, Daniels D, Huang H, Zhang Z. Detecting the H3F3A mutant allele found in high-grade pediatric glioma by real-time PCR. *J Neurooncol*. 2016;126(1):27-36. https://doi.org/10.1007/s11060-015-1936-5

23 Guo J, Zhang R, Yang Z, Duan Z, Yin D, Zhou Y. Biological Roles and Therapeutic Applications of IDH2 Mutations in Human Cancer. *Front Oncol*. 2021;11:644857. Published 2021 Apr 26. https://doi.org/10.3389/fonc.2021.644857

24 Zhang C, Xiao J, Fa L, et al. Identification of co-expressed gene networks promoting $CD8^+$ T cell infiltration and having prognostic value in uveal melanoma. *BMC Ophthalmol*. 2023;23(1):354. Published 2023 Aug 10. https://doi.org/10.1186/s12886-023-03098-7

25 Thomis DC, Berg LJ. The role of Jak3 in lymphoid development, activation, and signaling. *Curr Opin Immunol*. 1997;9(4):541-547. https://doi.org/10.1016/s0952-7915(97)80108-2

26 Benhassine M, Le-Bel G, Guérin SL. Contribution of the STAT Family of Transcription Factors to the Expression of the Serotonin 2B (HTR2B) Receptor in Human Uveal Melanoma. *Int J Mol Sci*. 2022;23(3):1564. Published 2022 Jan 29. https://doi.org/10.3390/ijms23031564

27 Schoenfield L, Janse S, Kline D, Aronow ME, Singh AD, Craven C, Abdel-Rahman M, Cebulla CM. Estrogen Receptor Is Expressed in Uveal Melanoma: A Potential Target for Therapy. Ocul Oncol Pathol. 2021 Sep;7(4):303-310. https://doi.org/10.1159/000512174. Epub 2021 May 7. PMID: 34604204; PMCID: PMC8443923.

28 Tanaka R, Terai M, Londin E, Sato T. The Role of HGF/MET Signaling in Metastatic Uveal Melanoma. Cancers (Basel). 2021 Oct 30;13(21):5457. https://doi.org/ 10.3390/cancers13215457. PMID: 34771620; PMCID: PMC8582360.